

Carlos Alfredo Contreras-Vargas
Fernando Israel Gómez-Castro*
Eduardo Sánchez-Ramírez
Juan Gabriel Segovia-Hernández
Ricardo Morales-Rodríguez
Zeferino Gamiño-Arroyo

Alternatives for the Purification of the Blend Butanol/Ethanol from an Acetone/Butanol/Ethanol Fermentation Effluent

Biobutanol is a biofuel with potential to substitute gasoline. It can be generated through fermentation of lignocellulosic material, by which acetone, butanol, and ethanol (ABE) are obtained and subsequently separated. Nevertheless, the blend ethanol/butanol itself is a fuel, so its separation could be not even necessary. An alternative is proposed to simplify the purification step of the ABE mixture, avoiding the separation of the ethanol/butanol blend. Intensification alternatives are suggested for the resulting structure. The proposed schemes are optimized through a stochastic approach, minimizing the total annual cost and the eco-indicator 99. The individual risk index is computed for selected designs. The suggested designs reduce the individual risk index by around 30–66 %.

Keywords: Alcohol blends, Biofuels, Gasoline substitution, Lignocellulose fermentation

Received: November 12, 2018; *revised:* December 24, 2018; *accepted:* March 04, 2019

DOI: 10.1002/ceat.201800641

1 Introduction

To reduce the dependency on fossil fuels, renewable substitutes, known as biofuels, have been developed during the last years. Such biofuels must have lower environmental impact than fossil fuels. Among liquid biofuels, bioalcohols are one kind of widely known renewable fuels, with bioethanol being the most popular. Bioethanol is obtained from raw materials composed mainly of cellulose and hemicellulose, e.g., corn, sugar cane, lignocellulosic wastes, among others. The production of bioethanol implies a pretreatment, when lignocellulosic material is used, followed by hydrolysis and fermentation stages, which may occur simultaneously [1, 2].

For the downstream process to purify bioethanol, several technologies have been applied either using conventional arrangements [3] or more complex topologies like extractive distillation and their intensified derivatives [4–6]. Another promising bioalcohol is biobutanol, which has better physical properties than bioethanol and, in some cases, even better than those of gasoline. Tab. 1 lists the main properties for the two bioalcohols and gasoline [7].

According to Tab. 1, butanol has a cetane number much higher than those of gasoline and ethanol, with an octane number comparable to the higher value for gasoline. The autoignition temperature is higher than that of gasoline, while the flash point is higher than that of gasoline and ethanol, making it a safer fuel. Moreover, the lower heating value of *n*-butanol is higher than that of ethanol. Other advantages of *n*-butanol over ethanol is that the first one is less soluble in water and can be mixed with gasoline at any proportion for its usage as fuel [8].

Biobutanol is obtained through the fermentation of renewable raw materials, particularly lignocellulosic biomass, e.g.,

Table 1. Physical properties for bioalcohols and gasoline [1].

	Gasoline	Ethanol	<i>n</i> -Butanol
Cetane number	0–10	8	25
Octane number	80–99	108	96
Autoignition temperature [°C]	~ 300	434	385
Flash point [°C]	–45 to –38	8	35
Lower heating value [MJ kg ⁻¹]	42.7	26.8	33.1
Latent heating at 25 °C [kJ kg ⁻¹]	380–500	904	582
Density at 20 °C [g mL ⁻¹]	0.72–0.78	0.79	0.81
Viscosity at 40 °C [mm ² s ⁻¹]	0.4–0.8 (20 °C)	1.08	2.63

sorghum straw, wheat straw, etc., giving a second use to these waste materials. One of the most frequently applied processes to produce biobutanol is the acetone, butanol, and ethanol (ABE) fermentation, which makes use of *Clostridium* strains to obtain *n*-butanol, with acetone and ethanol as byproducts. Such strains allow using hexoses and pentoses for fermenta-

Carlos Alfredo Contreras-Vargas, Dr. Fernando Israel Gómez-Castro, Dr. Eduardo Sánchez-Ramírez, Prof. Juan Gabriel Segovia-Hernández, Dr. Ricardo Morales-Rodríguez, Dr. Zeferino Gamiño-Arroyo, fgomez@ugto.mx

Universidad de Guanajuato, Campus Guanajuato, División de Ciencias Naturales y Exactas, Departamento de Ingeniería Química, Noria Alta S/N Col. Noria Alta, 36050 Guanajuato, México.

tion, which are contained in the lignocellulosic materials. Nevertheless, the ABE fermentation has low yields, resulting in low concentrations for the products, which is a common issue in the production of alcohols from biomass [9]. To enhance the process, the application of integrated fermentation-saccharification reactors has been proposed [10].

A second important challenge in this process is the purification of butanol, since the stream leaving the fermentation stage is diluted, with a water composition close to 80 wt % [11]. Moreover, the composition of the effluent is in the region where a homogeneous azeotrope ethanol-water and a heterogeneous azeotrope butanol-water occur. The previously mentioned factors make the separation of butanol, ethanol, and acetone into pure components more difficult, thereby increasing the energetic requirements and the capital costs of the purification step if conventional distillation is used. A conventional scheme is illustrated in Fig. 1 a, where in column C1 excess water is separated as bottom products. In column C2 acetone is obtained as distillate, together with a small proportion of the other components. Column C3 is used to completely purify acetone in the distillate, while the bottom stream contains traces of ethanol, butanol, and water. The decanter D1 is used to handle the heterogeneous azeotrope, helping to obtain water in the bottom of column C4 and butanol in the bottom of column C5.

Some alternatives proposed for the separation of such mixtures involve adsorption [12], pervaporation [13], and hybrid configurations with liquid-liquid extraction [14, 15]. Nevertheless, adsorption has been tested only at laboratory scale. On the other hand, the use of pervaporation membranes is still limited by its cost. The application of a hybrid sequence seems to be a promising alternative for the separation of the ABE mixture, as reported for the purification of other bioalcohols [16, 17]. Such separation train is displayed in Fig. 1 b, where a liquid-liquid extraction column is first used to remove the water from the beginning. Sánchez-Ramírez et al. [14] reported that such separation train requires the lowest total annual cost compared to the conventional sequence.

In a recent work, it has been demonstrated that the blend butanol/ethanol can be used as fuel to run internal combustion engines, with only slight variations in the main performance parameters of the engine, i.e., effective power, torque and specific fuel consumption, in comparison with neat butanol [18]. This implies that the separation of the binary mixture ethanol/butanol from the ABE fermentation is not necessary. Thus, in this work, a simplified separation scheme is proposed to purify the ABE mixture, aiming to obtain as products acetone and the blend ethanol/butanol. The hybrid structure shown in Fig. 1 b is taken as basis to propose a reduced separation train. To further reduce heating requirements, energy-efficient schemes are obtained from the reduced train. All the proposed structures are then optimized in terms of total annual cost and environmental impact, to find the designs with the better commitment between those objectives.

Differential evolution with the Tabu list is used as optimization algorithm. Moreover, safety indexes are computed for the optimized designs since the industry in the 21st century demands not only low-cost, but also environmentally friendly and inherently safe processes.

2 Case Study

The flow rate and composition of the stream entering the purification train are first computed. It has been assumed that 21 115 kg h⁻¹ of lignocellulosic material is fed to the fermentation step, with 40 wt % water. Thus, the solid fraction has a mass flow rate of 12 130 kg h⁻¹, with 45 wt % cellulose, 30 wt % hemicellulose, and 25 wt % lignin. According to Quiroz-Ramírez et al. [19] and Qureshi et al. [20], the yield for the fermentation step in the biobutanol process is 0.308675 kg ABE per kg biomass. Moreover, a ratio of 3:6:1 has been reported for the produced acetone, butanol, and ethanol [21]. With this information, the data in Tab. 2 are computed, at 34 °C and 1 bar. It is evident that the water is the component with the higher composition in the mixture to be separated.

It is desired to recover 98 wt % of each component, with a purity of 99 wt % for the pure acetone and ethanol, and 99.5 wt % for pure butanol. In the case of the blend ethanol/butanol, the purity of butanol is around 85 wt %, but the recovery of the alcohols is taken as the design goal for such stream.

Table 2. Data for the stream entering the purification train.

Component	Symbol	Flow rate [kg h ⁻¹]	Mass fraction [%]
Acetone	A	842.45	7.14
Butanol	B	1684.90	14.29
Ethanol	E	280.82	2.38
Water	W	8985.00	76.19

3 Methodology

3.1 Preliminary Design

The initial design of the studied systems has been performed through simulations in Aspen Plus V. 8.8. Previous works report that the phase equilibrium of the studied system can be represented with proper accuracy through the NRTL-HOC equation [14, 15, 22]; thus, this model was selected for this work. For comparison purposes, the hybrid train with a liquid-liquid extraction column (hybrid sequence, HS) reported by Sánchez-Ramírez et al. [14] is simulated (Fig. 1 b). For the liquid-liquid extraction column, hexyl acetate is used as extractant [14]. As a first approach, the values of the design variables are taken from the work of Sánchez-Ramírez et al. [14], adjusting the operational variables, i.e., mainly reflux ratio and heat duties, to reach the desired recoveries and purities. This purification train allows obtaining acetone, butanol, and ethanol as products. In this work, reduced trains are proposed, aiming to obtain acetone as pure product, and the fuel blend ethanol/butanol.

The first reduced sequence is achieved by eliminating column C4 from the HS, resulting in the system indicated in Fig. 2. Since only the last column of the HS is eliminated, the design and operational variables for the remaining columns are the same than those corresponding to the columns C1, C2, and

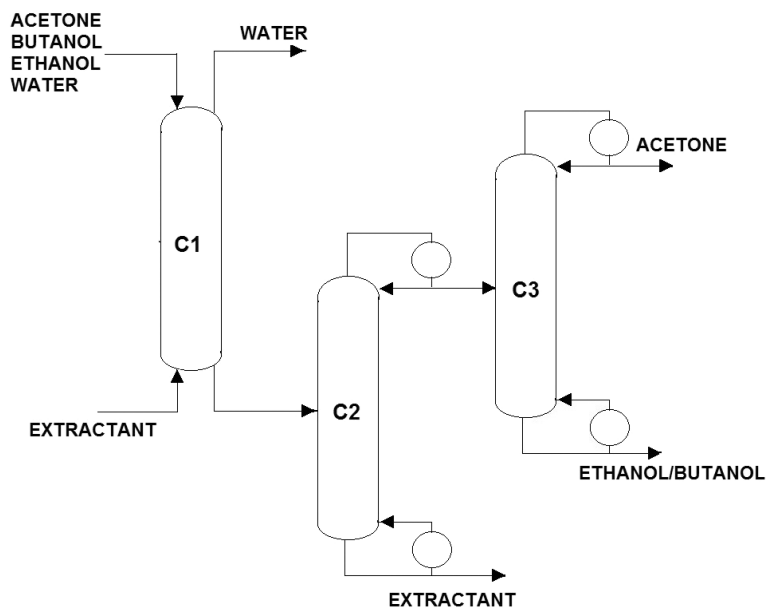


Figure 2. Reduced hybrid sequence (RHS) for the separation of the ABE mixture.

where only columns C2 and C3 are presented since the liquid-liquid extraction column (C1) remains the same for all cases.

The second modified system is a thermodynamically equivalent sequence (TES, Fig. 3 c), whose design is obtained by moving the rectification section (section III) of column C3 in the TCS to the top of column C2, linking the resulting structure with the stripper section of column C3 of the TCS through the streams FL1 and FV1. The third system is an intensified sequence (IS, Fig. 3 d). The design for the intensified sequence is achieved by eliminating section IV in the TCS, replacing it by a side stream.

Another system proposed for the separation of the ABE mixture is a dividing-wall column, here represented as a Petlyuk column (PC, Fig. 4 b). This sequence is designed from a three-column conventional sequence (C2, C3, and C4 in Fig. 4 a), whose design parameters are obtained through short-cut methods, using the DSTWU module of Aspen Plus. Then, stages are rearranged, turning column C2 of the three-column sequence into the prefractionator

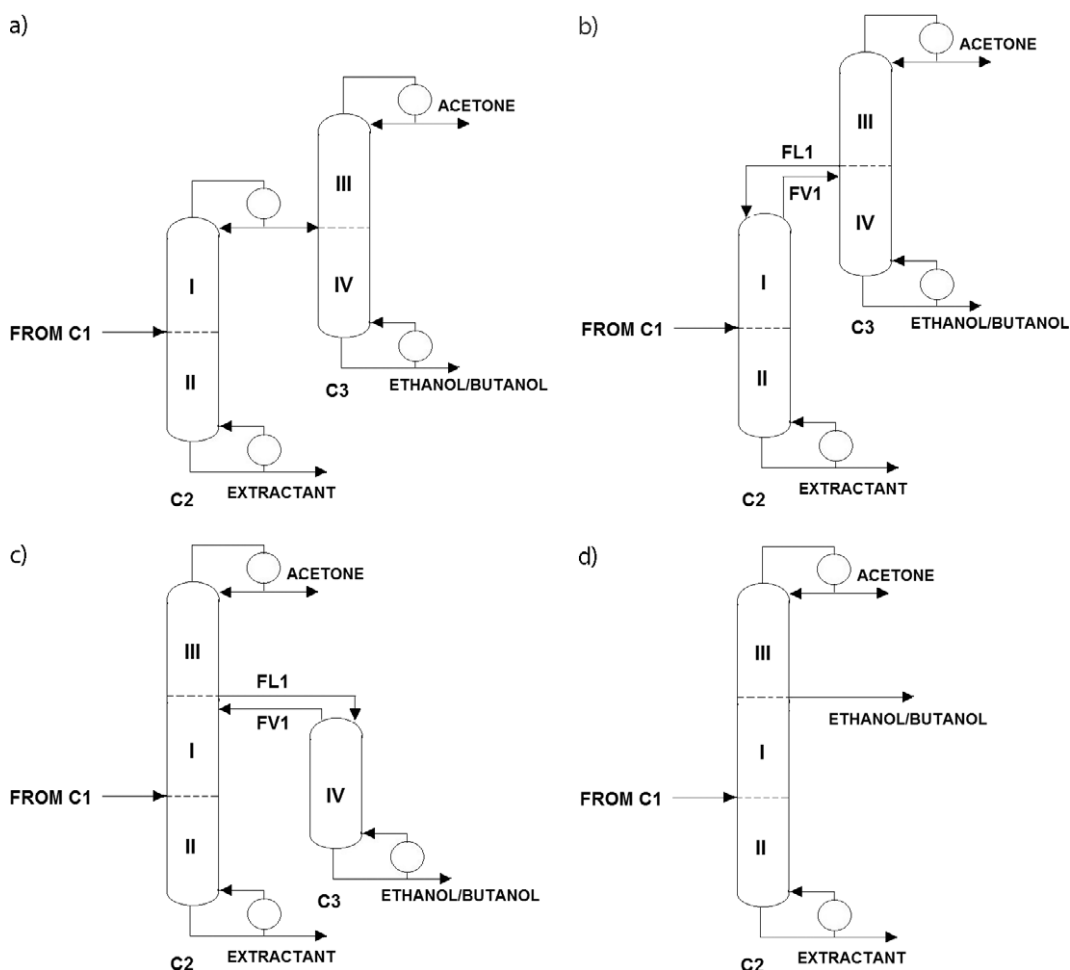


Figure 3. (a) Distillation sections of the reduced hybrid sequence, (b) thermally coupled sequence (TCS), (c) thermodynamically equivalent sequence (TES), (d) intensified sequence (IS).

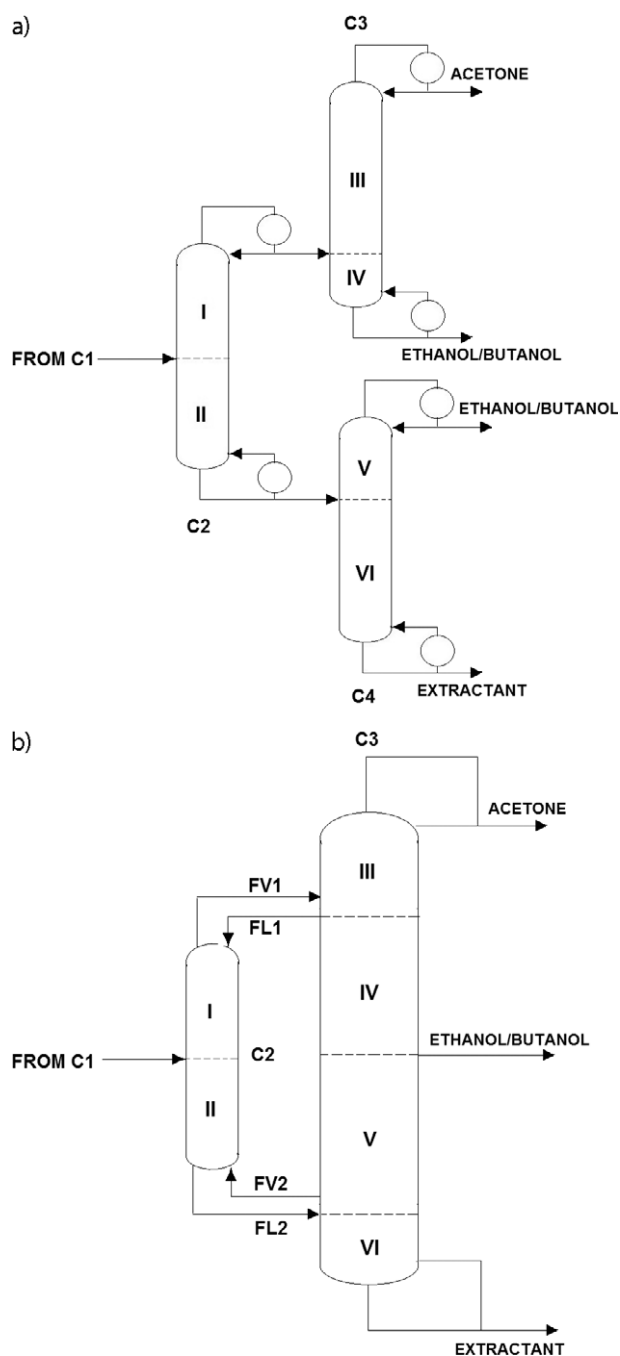


Figure 4. (a) Conventional sequence for the design of a Petlyuk column, (b) Petlyuk column (PC).

of the Petlyuk column, and columns C3 and C4 of the conventional three-column sequence into the main column of the Petlyuk column (C3).

3.2 Optimization

Taking the preliminary designs as initial solutions, an optimization strategy is applied to obtain a set of optimal designs

which accomplish the design specifications. A multi-objective optimization approach is considered, aiming to simultaneously minimize the total annual cost (TAC) and the environmental impact of each sequence. Thus, the optimization problem can be stated as follows:

$$\begin{aligned} \min_{\bar{x}} \bar{Z} &= [TAC, EI99] \\ \text{s.t.} & \\ h_i(\bar{x}) &= 0 \\ g_j(\bar{x}) &= x_j - y_j \leq 0 \end{aligned} \tag{1}$$

\bar{Z}^1 is the vector of objective functions, composed by the TAC and the measurement of the environmental impact (EI99), $h_i(\bar{x})$ are the equalities constraints, which are given by the model of the systems (mass balances, energy balances, equilibrium relationships, etc.), $g_j(\bar{x})$ are the inequalities constraints, while x_j and y_j are the required and obtained purity for the component j , respectively. Finally, \bar{x} is the vector of decision variables, which are different for each case. Tab. 3 summarizes all decision variables, process constraints, and objective functions used in the optimization process for the alternatives evaluated.

Table 3. Inequality constraints, decision variables, and objective function.

Variable/type of variable	Search range	
Number of stages	Discrete	5–100
Feed stages	Discrete	4–99
Side stream stage	Discrete	4–99
Side stream flow	Continuous	0.1–12 000 kg h ⁻¹
Reflux ratio	Continuous	0.5–75
Liquid and vapor interlinking flow	Continuous	0.1–12 000 kg h ⁻¹
Distillate rate	Continuous	0.1–12 000 kg h ⁻¹
Diameter	Continuous	0.9–5 m
Process constrains		
Purity	Acetone	> 99 wt %
	Butanol	> 99.5 wt %, > 85 wt % (blend)
	Ethanol	> 99 wt %, < 15 wt % (blend)
Recovery	Acetone	> 98 wt %
	Butanol	
	Ethanol	
Objective function		
Total annual cost (Eq. (2))		
Eco-indicator 99 (Eq. (3))		

1) List of symbols at the end of the paper.

3.2.1 Economic Performance Index

To evaluate the economic impact of the proposed alternatives, the TAC is taken as economic index. TAC calculation is based on the method previously reported by Guthrie [24], using the update reported by Turton et al. [25]. In general terms, the method consists in calculating the cost of an industrial plant in terms of the cost of separated units, computing the TAC as the sum of the annualized capital cost and the operating cost:

$$TAC = \frac{\text{Capital costs}}{\text{Payback Period}} + \text{Operating Costs} \quad (2)$$

In this work, a payback period of ten years is assumed, with 8500 operating hours per year. In addition, the following heating and cooling unitary costs were used: high-pressure (HP) steam (42 bar, 254 °C, 9.88 USD GJ⁻¹), medium-pressure (MP) steam (11 bar, 184 °C, 8.22 USD GJ⁻¹), low-pressure (LP) steam (6 bar, 160 °C, 7.78 USD GJ⁻¹), and cooling water (0.72 USD GJ⁻¹) [26].

3.2.2 Environmental Performance Index

The environmental impact is evaluated through the eco-indicator 99 (EI99), which is a life-cycle assessment (LCA) methodology to evaluate products and processes. This LCA methodology allows evaluating the environmental loads associated with a process, activity or product. Due to environmental concerns, some researchers have introduced this methodology to measure and improve the environmental performance of production processes, e.g., Alexander et al. [27] and Gebreslassie et al. [28].

In this methodology, 11 impact categories are considered, which are classified into three major damage categories: (1) human health, (2) ecosystem quality, and (3) resources depletion. In this work, the impact of the most important factors in the process is evaluated: the steam used to heat the bottoms of the columns, the electricity for pumping, and the production of the steel used to build the major equipment and accessories. Thus, the amount of steam, steel, and electricity used in each process is multiplied by the corresponding impact factor of each of these 11 categories; the factors are listed in Tab. 4.

The data associated with these upstream activities generally are taken from standard databases [29]. The scale was developed in such a way that the value of 1 point is representative for 1/1000 of the yearly environmental load of one average European inhabitant [29]. The EI99 is then defined as follows:

$$EI99 = \sum_b \sum_d \sum_{k \in K} \delta_d \omega_d \beta_b \alpha_{b,k} \quad (3)$$

β_b represents the total amount of chemical b released per unit of reference flow due to direct emissions, $\alpha_{b,k}$ is the damage caused by category k per unit of chemical b released to the environment, ω_d is a weighting factor for damage in category d , and δ_d is the normalization factor for damage of category d .

Table 4. Unitary values of eco-indicator used to measure the eco-indicator 99 in the studied systems [29].

Impact category	Steel [points kg ⁻¹]	Steam [points kg ⁻¹]	Electricity [points kWh ⁻¹]
Carcinogenics	6.32×10^{-3}	1.18×10^{-4}	4.36×10^{-4}
Climate change	1.31×10^{-2}	1.60×10^{-3}	3.61×10^{-6}
Ionizing radiation	4.51×10^{-4}	1.13×10^{-3}	8.24×10^{-4}
Ozone depletion	4.55×10^{-6}	2.10×10^{-6}	1.21×10^{-4}
Respiratory effects	8.01×10^{-2}	7.87×10^{-7}	1.35×10^{-6}
Acidification	2.71×10^{-3}	1.21×10^{-2}	2.81×10^{-4}
Ecotoxicity	7.45×10^{-2}	2.80×10^{-3}	1.67×10^{-4}
Land occupation	3.73×10^{-3}	8.58×10^{-5}	4.68×10^{-4}
Fossil fuels	5.93×10^{-2}	1.25×10^{-2}	1.20×10^{-3}
Mineral extraction	7.42×10^{-2}	8.82×10^{-6}	5.70×10^{-6}

3.3 Global Optimization Methodology

To perform the multi-objective optimization, the differential evolution with Tabu list (DETL) method is used. Differential evolution (DE) was proposed by Storn and Price [30] for a single-objective function and adapted by Madavan et al. [31] to solve multi-objective problems. The DE algorithm involves five steps: initialization, mutation, crossover, evaluation, and selection [30]. The Tabu list concept (TL) and Tabu Search (TS) were proposed by Glover et al. [32]. Both strategies allow avoiding revisit the search space by keeping a record of previously visited points. DETL combines the DE optimization algorithm with the concept of TL.

The global optimization strategy was developed using a hybrid platform which links Aspen Plus and Microsoft Excel. In Microsoft Excel, the DETL algorithm is written with Visual Basic and the separation scheme is modeled in Aspen Plus. To start with the DETL algorithm, it is necessary to propose an initial vector. Before its evaluation in the model, it is necessary to call a subroutine to open the Aspen Plus interface, where the previously proposed vector is evaluated. As a result, Aspen Plus provides several output data (reboiler/condenser heat duties, purities, flow rates, etc.). A lot of the output data is used to evaluate the objective functions, e.g., both the column sizing and reboiler heat duties are taken to calculate the TAC and the EI99. On the other hand, some output data are used to guide the algorithm to improve the optimization process.

Once the objective functions are calculated in Microsoft Excel, those cells return the information to the DETL algorithm. The optimization method analyzes the objective function values and proposes new values for the decision variables according to the DETL methodology. Microsoft Excel and its interface allow the user to recalculate the values proposed by the DETL method. In this way, it is possible to ensure the assignment of integer values to the integer process variables, e.g., feed loca-

tion, through the command 'round up', avoiding the selection of non-integer values for these variables. The parameters for the optimization process were: 200 individuals, maximum number of generations of 1000, a Tabu list of 50 % of total individuals, a Tabu radius of 1×10^{-6} , and 0.8 and 0.6 for crossover probability and mutation factor, respectively. These parameters were obtained from the literature [20] and by a tuning process from preliminary calculations.

The proposed separation systems are optimized in the following order: first, the hybrid sequence and the reduced hybrid sequence are optimized, taking as decision variables the number of stages and the flow rate of the extractant for the liquid-liquid extraction column, and the total number of stages of each column and the feed stages for the distillation columns. Then, the TCS and the TES are optimized in terms of the interlinking flow rates, reflux ratios, and either bottoms or distillate flows, while the intensified sequence (IS) is optimized using reflux ratio and side stream flow as decision variables. The number of stages of these three energy-efficient sequences is directly obtained by stage rearrangement from the optimal designs of the RHS, following the arguments of Errico et al. [33], which conclude that the optimal structure for the sections of the modified structures is the same as the optimal structure of the sections of the conventional sequence from where they are derived. Finally, the Petlyuk column is optimized taking as decision variables the total number of stages for the prefractionator and the main column, respectively, the location of the feed streams, and the flow rates of the interlinking streams FL1 and FV2.

3.4 Individual Risk Index

The risk is quantified by means of the individual risk (IR). The IR can be defined as the risk of injury or decease to a person in the neighborhood of a hazard [34]. The main objective of this index is the estimation of the likelihood of affectation caused by the specific incident that occurs with a certain frequency. The IR does not depend on the number of people exposed. The mathematical expression for calculating the individual risk is the following:

$$IR = \sum f_i P_{x,y} \quad (4)$$

f_i is the occurrence frequency of incident i , whereas $P_{x,y}$ is the probability of injury or decease caused by the incident i . In this work, irreversible injuries (decease) are studied, for which more data are recorded. The calculation of IR can be carried out through quantitative risk analysis (QRA), which is a methodology to assess potential incidents and accidents and their consequences. As first step, the QRA identifies possible incidents for the system under analysis. Regarding distillation columns, the incidents could be either instantaneous or continuous releases. A continuous release is mainly produced by a rupture in a pipeline or partial rupture on a process vessel, causing a leak. The instantaneous release consists in the total loss of matter from the process equipment, originated by its catastrophic rupture.

Fig. 5 presents the event tree diagrams obtained with all the probabilities of instantaneous and continuous incidents, along with their respective frequencies. Once the incidents have been

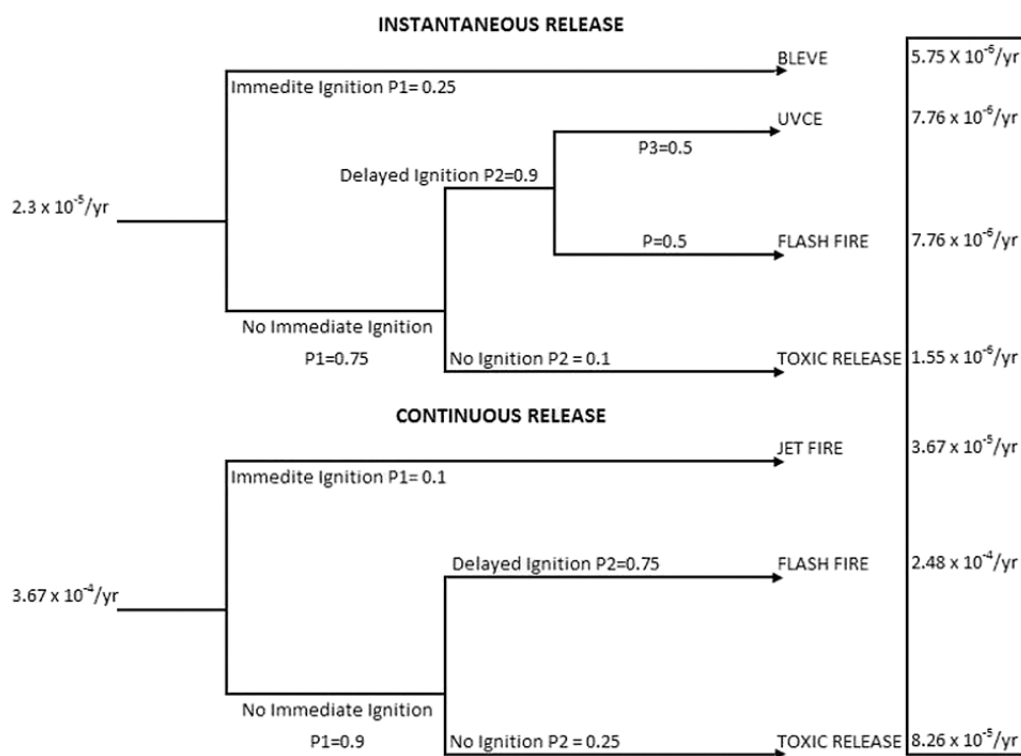


Figure 5. Event tree diagram.

identified, the probability $P_{x,y}$ can be calculated through a consequence assessment, which consists in determining the physical variables as the thermal radiation, the overpressure and the concentration of the leak originated by incidents, and their respective damages. In general, the calculation of the IR was realized according to the equations reported by many authors, e.g., Freeman [24] and Medina-Herrera et al. [35].

4 Results

Fig. 6a illustrates the solution profile for the hybrid sequence (HS), while Fig. 6b presents the solution profile for the RHS. For HS, once the optimization procedure is finished, values of $EI99$ range between 4 922 900 and 4 930 361 points a^{-1} , while TAC varies between 13 144 883 and 13 170 857 USD a^{-1} . In the case of the RHS, $EI99$ values are in the range of 4 894 093 to 4 895 372 points a^{-1} , while TAC lies between 13 032 616 and 13 046 675 USD a^{-1} . Thus, there is only a small deviation between the final solutions for the hybrid sequences. For each case, an equilibrium solution is taken from the solution profile, located in the mid-zone on the plot. For the HS, the equilibri-

um solution has an $EI99$ of 4 926 199 points a^{-1} and a TAC of 13 150 832 USD a^{-1} , while the RHS has an $EI99$ of 4 894 118 points a^{-1} and a TAC of 13 034 431 USD a^{-1} . This implies that eliminating the ethanol/*n*-butanol column would reduce the environmental impact and TAC by $\sim 0.65\%$ and 0.88% , respectively.

Fig. 7 presents the solution profiles for the sequences synthesized from the RHS. The solution profile of the TCS (Fig. 7a) shows designs with the $EI99$ ranging from 4 862 172 to 4 862 209 points a^{-1} and TAC values from 12 846 151 to 12 846 989 USD a^{-1} . Fig. 7b shows the solution profile for the TES; here, $EI99$ values are between 4 876 737 and 4 876 899 points a^{-1} , while TAC varies between 12 885 568 and 12 889 726 USD a^{-1} . Finally, the solution profile for the IS is displayed in Fig. 7c, where $EI99$ ranges from 5 478 435 to 5 478 960 points a^{-1} and TAC from 14 626 260 to 14 629 327 USD a^{-1} .

For each sequence, an equilibrium solution has been chosen. The selected solutions for the thermally coupled, thermodynamically equivalent and intensified sequences have values of 4 862 178, 4 876 762, and 5 478 604 points a^{-1} for $EI99$, and 12 846 215, 12 886 075 and 14 626 536 USD a^{-1} for TAC, respectively.

It is clear that among the three systems here analyzed the IS has the worst performance, showing higher values of $EI99$ and TAC even higher than the hybrid sequences. On the other hand, the TCS has the lowest $EI99$ and TAC, followed by the TES, with reductions of 1.29% and 1% for $EI99$ and 2.32% and 2.01% for TAC, regarding the hybrid sequence HS.

The solution profile for the Petlyuk column is given in Fig. 8. This sequence is analyzed apart from the others since it is synthesized from a different conventional sequence. For this system, $EI99$ ranges between 6 099 035 and 6 103 245 points a^{-1} , while TAC is in the range between 15 577 404 and 15 601 107 USD a^{-1} . The selected solution for this system has an $EI99$ of 6 100 390 points a^{-1} and TAC of 15 579 321 USD a^{-1} . This implies that the Petlyuk column has a bad performance for this separation, increasing the $EI99$ by 15.6% and the TAC in 19.2%, in comparison with the HS. This could be due to the relatively low composition of the light- and medium-boiling components, in comparison with the heavy component (hexyl acetate).

Tab. 5 summarizes the main characteristics of the selected equilibrium solutions from the profiles in Figs. 5–7, where HA represents

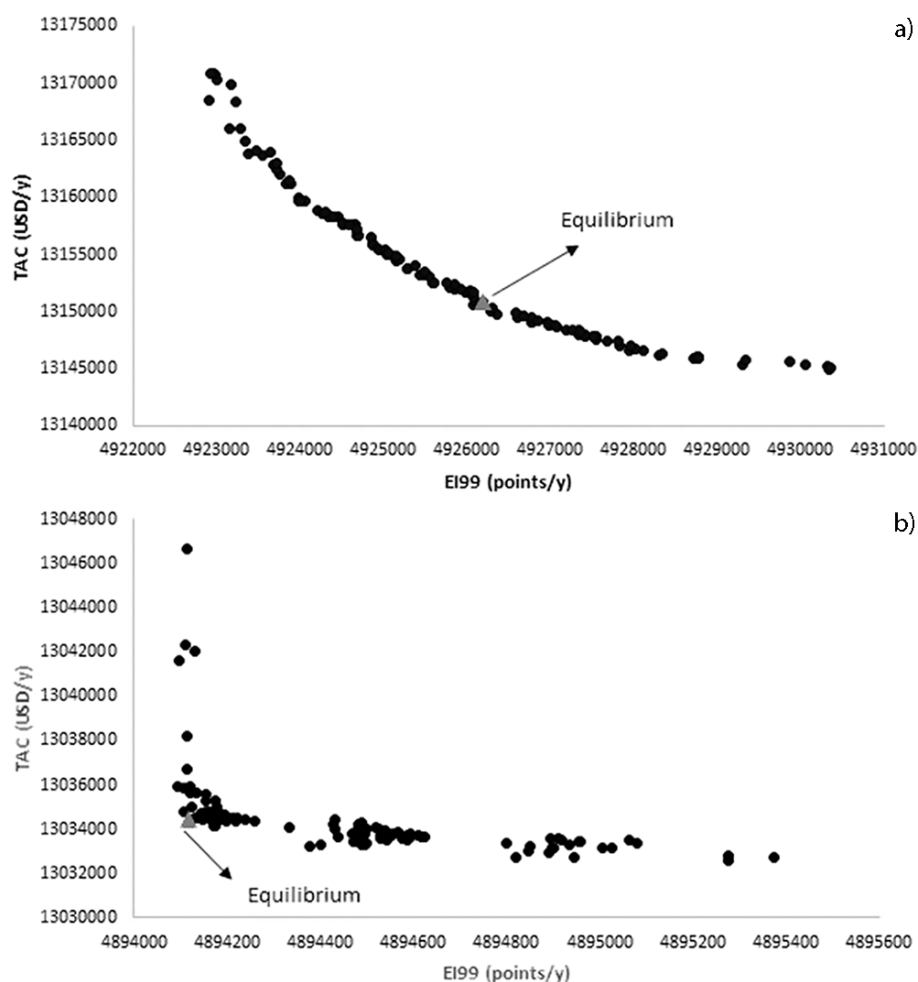


Figure 6. Solution profile (a) for the hybrid sequence HS, (b) for the reduced hybrid sequence RHS.

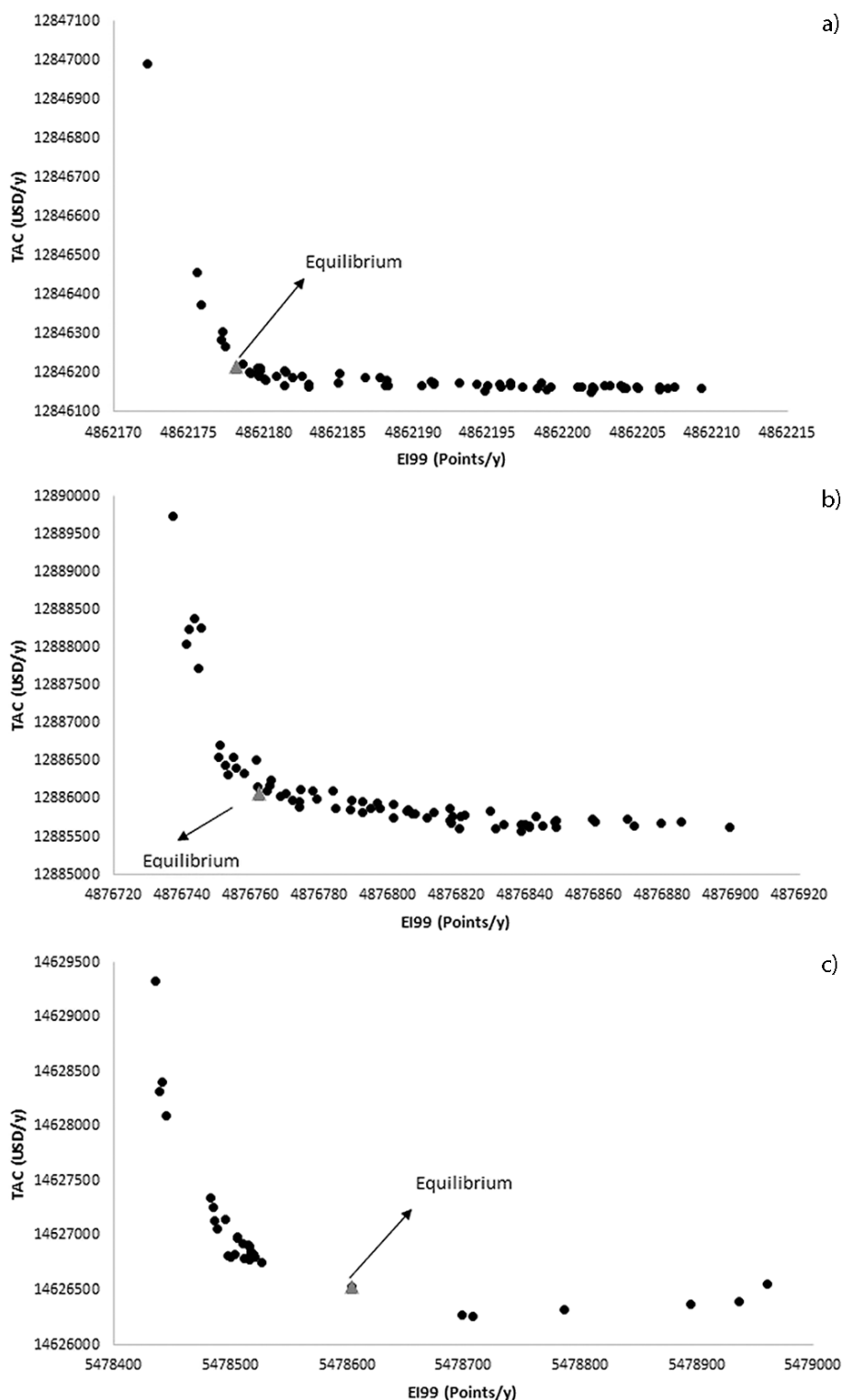


Figure 7. Solution profile (a) for the thermally coupled sequence TCS, (b) for the thermodynamically equivalent sequence TES, (c) for the intensified sequence ES.

hexyl acetate. Among the studied sequences, the IS reached a purity for butanol slightly below the desired value, while the other sequences achieved the desired purities. In terms of heat

duty, the HS, RHS, and TCS require total duties below 28 500 kW. On the other hand, the TES, IS, and PC require total heat duties higher than 30 000 kW. It is observed that the column C2 in HS and RHS, in which the solvent is recovered, has the higher contribution to the total heat duty, namely, > 98 %, which can explain the small effect of the elimination of the last column in the TAC and in the EI. This indicates that in order to further diminish the total energy requirements of the sequences, the use of a different solvent may be necessary to reduce the solvent flow rate in the liquid-liquid extraction column but keeping the high removal of water.

- a) duty, the HS, RHS, and TCS require total duties below 28 500 kW. On the other hand, the TES, IS, and PC require total heat duties higher than 30 000 kW. It is observed that the column C2 in HS and RHS, in which the solvent is recovered, has the higher contribution to the total heat duty, namely, > 98 %, which can explain the small effect of the elimination of the last column in the TAC and in the EI. This indicates that in order to further diminish the total energy requirements of the sequences, the use of a different solvent may be necessary to reduce the solvent flow rate in the liquid-liquid extraction column but keeping the high removal of water.
- b)

Tab. 6 presents the results for the risk assessment of the distillation columns. Both yearly decrease probabilities due to exposure to an instantaneous release incident (BLEVE, UVCE, or instantaneous toxic release) and due to a continuous release incident (continuous toxic release or flash fire) are given for each equipment and for the whole sequence. Also, the individual risk index is reported, in terms of the kind of accident and its frequency. Note that the risk analysis for the Petlyuk column is only performed for the main column C3, since the prefractionator has neither energy requirements nor products. Tab. 6 demonstrates that the column in which the extractant is recovered is the most dangerous in terms of instantaneous release.

In the case of continuous release, no variation is found. Nevertheless, when the whole sequences are analyzed, it can be observed that eliminating the last column from the HS allows reducing the risk of continuous release by around 30 %, consequently decreasing the IR in a similar proportion. Moreover, when the number of distillation columns is decreased to one, as occurs with the IS and the Petlyuk column, the IR is reduced by around 66 % in comparison with the HS and by

Table 5. Optimal design characteristics for the selected points from the solution profiles.

	HS				RHS		
	C1	C2	C3	C4	C1	C2	C3
Number of stages	3	66	60	33	3	63	61
Feed stages	1, 3	61	23	13	1, 3	58	24
Reflux ratio	–	0.6	1.5	1.6	–	0.6	1.5
Heat duty [kW]	–	27 966.8	321.2	189.6	–	27 971.7	320.8
Extractant flow rate [kg h ⁻¹]	331 568	–	–	–	331 568	–	–
Product purity [wt %]	99.8 (W)	99.99 (HA)	99.6 (A)	99.6/99.9 (E/B)	99.8 (W)	99.99 (HA)	99.6/85.6 (A/B)
	TCS			TES			
	C1	C2	C3	C1	C2	C3	
Number of stages	3	63	61	3	87	37	
Feed stages	1, 3	1,55	24	1, 3	24, 58	1	
Reflux ratio	–	0.3	6.9	–	29.6	2.8	
Heat duty [kW]	–	27 914.9	210.9	–	30 602.5	187.9	
FL1 [kmol h ⁻¹]	–	20.8	20.8	–	44.4	44.4	
FV1 [kmol h ⁻¹]	–	63.5	63.5	–	15.6	15.6	
Extractant flow rate [kg h ⁻¹]	331 568	–	–	331 568	–	–	
Product purity [wt %]	99.8 (W)	99.99 (HA)	99.8/85.4 (A/B)	99.8 (W)	99.8/99.99 (A/HA)	85.6 (B)	
	IS			PC			
	C1	C2		C1	C2	C3	
Number of stages	3	87		3	21	99	
Feed stages	1, 3	56		1, 3	1, 18, 21	16, 52	
Reflux ratio	–	38.9		–	–	53.1	
Heat duty [kW]	–	31 799.1		–	–	33 595.0	
Side stream stage	–	24		–	–	19	
Side stream flow rate [kmol h ⁻¹]	–	29.1		–	–	28.8	
FL1 [kmol h ⁻¹]	–	–		–	4225.8	4225.8	
FV1 [kmol h ⁻¹]	–	–		–	1878.1	1878.1	
FL2 [kmol h ⁻¹]	–	–		–	331.7	331.7	
FV2 [kmol h ⁻¹]	–	–		–	326.2	326.2	
Extractant flow rate [kg h ⁻¹]	331 568	–		331 568	–	–	
Product purity [wt %]	99.8 (W)	99.1/84.8/99.99 (A/B/HA)		99.8 (W)	–	99.1/85.8/99.99 (A/B/HA)	

mental impact. On the other hand, the schemes TCS and TES have the lowest values for TAC and EI and intermediate values for IR, making these sequences the most balanced among the studied systems.

5 Conclusions

A proposal for enhancing the purification process of the ABE mixture is presented which implies avoiding the ethanol/butanol separation since this mixture can be used as fuel in internal combustion engines. Process flowsheets for conventional and

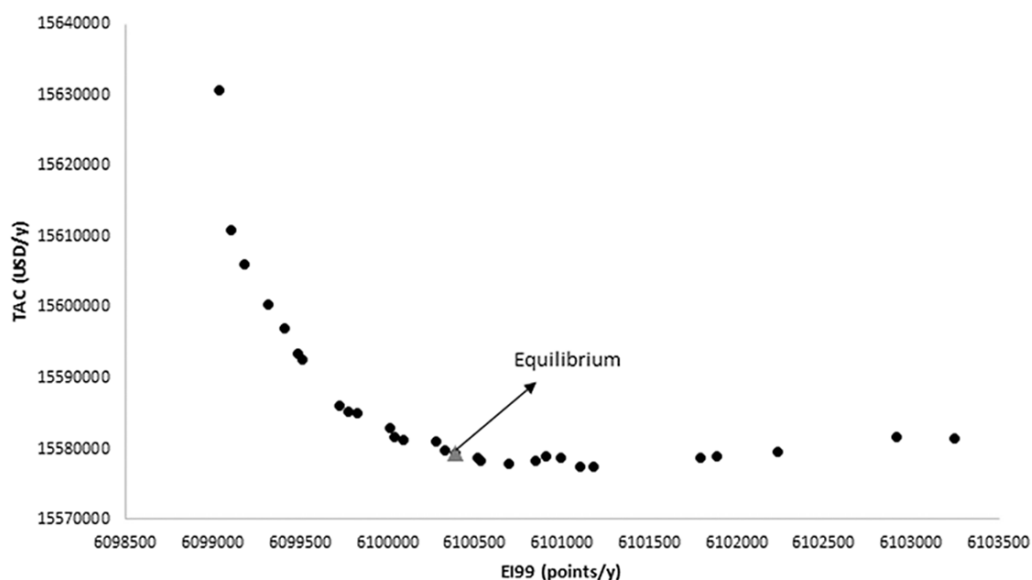


Figure 8. Solution profile for the Petlyuk column.

Table 6. Results for the risk analysis.

	HS			RHS	
	C2	C3	C4	C2	C3
Instantaneous (equipment)	1.4×10^{-5}	2.0×10^{-7}	6.7×10^{-8}	1.4×10^{-5}	2.1×10^{-7}
Continuous (equipment)	2.5×10^{-4}				
Instantaneous (sequence)	1.4×10^{-5}			1.4×10^{-5}	
Continuous (sequence)	7.5×10^{-4}			5.0×10^{-4}	
IR	7.7×10^{-4}			5.2×10^{-4}	
	TCS		TES		
	C2	C3	C2	C3	
Instantaneous (equipment)	1.4×10^{-5}	5.3×10^{-7}	1.4×10^{-5}	2.1×10^{-7}	
Continuous (equipment)	2.5×10^{-4}	2.5×10^{-4}	2.5×10^{-4}	2.5×10^{-4}	
Instantaneous (sequence)	1.4×10^{-5}		1.4×10^{-5}		
Continuous (sequence)	5×10^{-4}		5×10^{-4}		
IR	5.1×10^{-4}		5.1×10^{-4}		
	IS		PC		
	C2		C3		
Instantaneous (sequence)	1.4×10^{-5}		1.4×10^{-5}		
Continuous (sequence)	2.5×10^{-4}		2.5×10^{-4}		
IR	2.6×10^{-4}		2.6×10^{-4}		

intensified distillation trains are presented and optimized in terms of total annual cost and environmental impact, assessing the safety properties of each sequence. The sequences are compared with the previously reported train, in which ethanol and butanol are obtained as separated products, to assess the impact of the proposed modification on the studied indexes.

Eliminating the column with the task of separating the ethanol/butanol mixture has only little effect on the total annual cost and the environmental impact, since the column with the highest energy requirements is the one which recovers the solvent used to remove the water in the ABE mixture. Nevertheless, the reduction in the number of columns has a high impact on the safety of the process.

Acknowledgment

The authors acknowledge the support of the Universidad de Guanajuato for the development of this work.

The authors have declared no conflict of interest.

Symbols used

EI_{99}	[points a ⁻¹]	eco-indicator 99
f_i	[-]	occurrence frequency of incident i
IR	[a ⁻¹]	individual risk
$P_{x,y}$	[-]	probability of injury or decease caused by the incident i
TAC	[USD a ⁻¹]	total annual cost
x_j	[-]	required purity for the component j
y_j	[-]	obtained purity for the component j
Z	[-]	vector of objective functions

Greek letters

$\alpha_{b,k}$	damage caused by category k per unit of chemical b released to the environment
β_b	total amount of chemical b released per unit of reference flow due to direct emissions
δ_d	normalization factor for damage of category d
ω_d	weighting factor for damage in category d

Abbreviations

BLEVE	boiling liquid expanding vapor explosion
DETL	differential evolution with Tabu list
HP	high-pressure
HS	hybrid sequence
IS	intensified sequence
LCA	life cycle assessment
LP	low-pressure
MP	middle-pressure
PC	Petlyuk column
RHS	reduced hybrid sequence
TCS	thermally coupled sequence
TES	thermodynamically equivalent sequence
UVCE	unconfined vapor cloud explosion

References

- [1] M. Balat, H. Balat, C. Öz, *Prog. Energy Combust. Sci.* **2008**, *34* (5), 551–573. DOI: <https://doi.org/10.1016/j.pecs.2007.11.001>
- [2] C. Conde-Mejía, A. Jiménez-Gutiérrez, M. M. El-Halwagi, *Process. Saf. Environ.* **2012**, *90* (3), 189–202. DOI: <https://doi.org/10.1016/j.psep.2011.08.004>
- [3] M. Errico, B.-G. Rong, G. Tola, M. Spano, *Ind. Eng. Chem. Res.* **2013**, *52* (4), 1612–1619. DOI: <https://doi.org/10.1021/ie301828d>
- [4] M. Vázquez-Ojeda, J. G. Segovia-Hernández, S. Hernández, A. Hernández-Aguirre, A. A. Kiss, *Sep. Purif. Technol.* **2013**, *105*, 90–97. DOI: <https://doi.org/10.1016/j.seppur.2012.12.002>
- [5] M. Errico, B.-G. Rong, G. Tola, M. Spano, *Ind. Eng. Chem. Res.* **2013**, *52* (4), 1620–1626. DOI: <https://doi.org/10.1021/ie301829n>
- [6] A. A. Kiss, R. M. Ignat, *Sep. Purif. Technol.* **2012**, *98*, 290–297. DOI: <https://doi.org/10.1016/j.seppur.2012.06.029>
- [7] C. Jin, M. Yao, H. Liu, C. F. Lee, J. Li, *Renewable Sustainable Energy Rev.* **2011**, *15* (8), 4080–4106. DOI: <https://doi.org/10.1016/j.rser.2011.06.001>
- [8] N. Qureshi, T. C. Ezeji, *Biofuels Bioprod. Biorefin.* **2008**, *2* (4), 319–330. DOI: <https://doi.org/10.1002/bbb.85>
- [9] J. Haider, M. A. Qyum, A. Hussain, M. Yasin, M. Lee, *Biochem. Eng. J.* **2018**, *140*, 93–107. DOI: <https://doi.org/10.1016/j.bej.2018.09.002>
- [10] P. Andric, A. S. Meyer, P. A. Jensen, K. Dam-Johansen, *Biotechnol. Adv.* **2010**, *28* (3), 407–425. DOI: <https://doi.org/10.1016/j.biotechadv.2010.02.005>
- [11] M. Wu, M. Wang, J. Liu, H. Huo, *Biotechnol. Prog.* **2008**, *24* (6), 1204–1214. DOI: <https://doi.org/10.1002/btpr.71>
- [12] X. Yang, G. J. Tsai, G. T. Tsao, *Sep. Technol.* **1994**, *4* (2), 81–92. DOI: [https://doi.org/10.1016/0956-9618\(94\)80009-X](https://doi.org/10.1016/0956-9618(94)80009-X)
- [13] K. Y. Jee, Y. T. Lee, *J. Membr. Sci.* **2014**, *456*, 1–10. DOI: <https://doi.org/10.1016/j.memsci.2013.12.061>
- [14] E. Sánchez-Ramírez, J. J. Quiroz-Ramírez, J. G. Segovia-Hernández, S. Hernández, A. Bonilla-Petriciolet, *Ind. Eng. Chem. Res.* **2015**, *54*, 351–358. DOI: <https://doi.org/10.1021/ie503975g>
- [15] M. Errico, E. Sánchez-Ramírez, J. J. Quiroz-Ramírez, J. G. Segovia-Hernández, B.-G. Rong, *Comput. Chem. Eng.* **2016**, *84*, 482–492. DOI: <https://doi.org/10.1016/j.compchemeng.2015.10.009>
- [16] A. Avilés Martínez, J. Saucedo-Luna, J. G. Segovia-Hernández, S. Hernández, F. I. Gómez-Castro, A. J. Castro-Montoya, *Ind. Eng. Chem. Res.* **2012**, *51* (17), 5847–5855. DOI: <https://doi.org/10.1021/ie200932g>
- [17] J. Haider, G. R. Harvianto, M. A. Qyum, M. Lee, *ACS Sustainable Chem. Eng.* **2018**, *6* (11), 14901–14910. DOI: <https://doi.org/10.1021/acssuschemeng.8b03414>
- [18] R. Arce-Alejandro, J. F. Villegas-Alcaraz, F. I. Gómez-Castro, L. Juárez-Trujillo, E. Sánchez-Ramírez, M. Carrera-Rodríguez, R. Morales-Rodríguez, *Clean Technol. Environ. Policy* **2018**, *20* (8), 1929–1937. DOI: <https://doi.org/10.1007/s10098-018-1584-5>
- [19] J. J. Quiroz-Ramírez, E. Sánchez-Ramírez, S. Hernández, J. H. Ramírez-Prado, J. G. Segovia-Hernández, *Ind. Eng. Chem. Res.* **2017**, *56* (7), 1823–1833. DOI: <https://doi.org/10.1021/acs.iecr.6b04230>
- [20] N. Qureshi, B. C. Saha, B. Dien, R. E. Hector, M. A. Cotta, *Biomass Bioenergy* **2010**, *34* (4), 559–565. DOI: <https://doi.org/10.1016/j.biombioe.2009.12.024>
- [21] D. T. Jones, D. R. Woods, *Microbiol. Rev.* **1986**, *50* (4), 484–524.
- [22] A. B. Van der Merwe, H. Cheng, J. F. Görgens, J. H. Knoetze, *Fuel* **2013**, *105*, 451–458. DOI: <https://doi.org/10.1016/j.fuel.2012.06.058>
- [23] S. Hernández, A. Jiménez, *Trans. Inst. Chem. Eng.* **1986**, *74*, 357–362.
- [24] K. M. Guthrie, *Chem. Eng.* **1969**, *76*, 114–142.
- [25] *Analysis, Synthesis and Design of Chemical Processes*, 3rd ed. (Eds: R. Turton, R. C. Bailie, W. B. Whiting, J. A. Shaeiwitz), Pearson Education, London **2008**.
- [26] C. S. Bildea, R. György, E. Sánchez-Ramírez, J. J. Quiroz-Ramírez, J. G. Segovia-Hernandez, A. A. Kiss, *J. Chem. Tech-*

- nol. Biotechnol.* **2015**, *90* (6), 992–1001. DOI: <https://doi.org/10.1002/jctb.4683>
- [27] B. Alexander, G. Barton, J. Petrie, J. Romagnoli, *Comput. Chem. Eng.* **2000**, *24* (2–7), 1195–1200. DOI: [https://doi.org/10.1016/S0098-1354\(00\)00356-2](https://doi.org/10.1016/S0098-1354(00)00356-2)
- [28] B. H. Gebreslassie, G. Guillén-Gosálbez, L. Jiménez, D. Boer, *Appl. Energy* **2009**, *86* (26), 1712–1722. DOI: <https://doi.org/10.1016/j.apenergy.2008.11.019>
- [29] M. Goedkoop, R. Spriensma, *The Eco-Indicator 99: A Damage-Oriented Method for Life Cycle Impact Assessment. Methodology Annex*, Product Ecology Consultants, Amersfoort **2001**.
- [30] R. Storn, K. Price, *J. Global Optim.* **1997**, *11* (4), 341–359. DOI: <https://doi.org/10.1023/A:1008202821328>
- [31] N. K. Madavan, *Proc. of the 2002 Congress on Evolutionary Computation* **2002**, *2*, 1145–1150.
- [32] F. Glover, *ORSA J. Comput.* **1989**, *1* (3), 135–206. DOI: <https://doi.org/10.1287/ijoc.1.3.190>
- [33] M. Errico, B. G. Rong, G. Tola, I. Turunen, *Chem. Eng. Process.* **2009**, *48* (4), 907–920. DOI: <https://doi.org/10.1016/j.cep.2008.12.005>
- [34] R. A. Freeman, *Plant/Operations Progress* **1990**, *9* (4), 231–235. DOI: <https://doi.org/10.1002/prsb.720090409>
- [35] N. Medina-Herrera, A. Jiménez-Gutiérrez, M. S. Mannan, *J. Loss Prevent. Proc.* **2014**, *29*, 225–239. DOI: <https://doi.org/10.1016/j.jlp.2014.03.004>